Capillary condensation for quantum fluids

M. Mercedes Calbi
Department of Physics and Center for Materials Physics, Pennsylvania State University, University Park, Pennsylvania 16802 and Departamento de Física, Universidad de Buenos Aires, Buenos Aires 1428, Argentina

Flavio Toigo
INFM, Istituto Nazionale per la Fisica della Materia and Dipartimento di Fisica ''Galileo Galilei,'' Università di Padova, 35100 Padova, Italy

Silvina M. Gatica
Department of Physics and Center for Materials Physics, Pennsylvania State University, University Park, Pennsylvania 16802 and Departamento de Física, Universidad de Buenos Aires, Buenos Aires 1428, Argentina

Milton W. Cole*
Department of Physics and Center for Materials Physics, Pennsylvania State University, University Park, Pennsylvania 16802
(Received 18 June 1999)

A simple model has been proposed and evaluated to predict the nature of capillary condensation in a slab geometry. We present a study of adsorption of fluids ^{3}He and ^{4}He that test this model. These calculations employ the density-functional method applicable at zero temperature. Overall, the simple model works well in comparison with microscopic calculations. [S0163-1829(99)01945-1]

I. INTRODUCTION

The phenomenon of capillary condensation (CC) has been the subject of extensive experimental and theoretical study, extending over many decades.[1–12] Nevertheless, there remain important questions about the validity of alternative interpretations of the various phenomena. For example, some models assume that the hysteresis observed experimentally originates in the kinetics of fluid transport, which is certainly constrained by the constrictions present in most porous media. Other models assume that the hysteresis is inherent in a first-order transition and is explicable in equilibrium terms as a result of the competition of locally stable states. In either case, regular geometries (e.g., slab or cylindrical geometry) have often been assumed in theoretical treatments. Most models rely on simplifying assumptions about the adsorption potentials and/or use macroscopic arguments, such as those that appear in the derivation of the venerable Kelvin equation.

Particular sources of current interest in this problem are the appearance of experimental data available for adsorption within well-characterized nanomaterials such as carbon nanotubes and zeolites. In such circumstances of extreme capillarity one should realize that macroscopic models are particularly fallible. Nevertheless, such models may provide reliable qualitative guides if used judiciously.

Recently [in a paper called GCC henceforth (where GCC is Gatica, Calbi, and Cole)], we have explored such a macroscopic model.[3] The virtue of such a simple model is obvious but it is essential to check whether the system of interest really exhibits the predicted behavior. That is a motivation for the present study. Our ''simple model'' analyzes the thermodynamics of adsorption in a slab geometry (separation L) in terms of bulk properties (surface tension σ and number density n) and the adsorption potential presented by the substrate. This model yields a kind of universal ''phase diagram'' of CC behavior. The specific equilibrium phase is found to depend in a simple way on the well depth of the adsorption potential D^*, the reduced difference Δ between the chemical potential and its value at saturation $(\mu-\mu_0)$, and the reduced separation L^* of the solid bodies confining the adsorbed fluid. These reduced quantities are defined by the following relations:

$$L^* = L/z_m, \tag{1}$$

$$\Delta = (\mu_0-\mu) n z_m/\sigma, \tag{2}$$

$$D^* = 2nDz_m/\sigma. \tag{3}$$

Here we are considering the case of a 3–9 potential arising from each of the neighboring surfaces,

$$V(z) = [4C^3/(27D^2)]z^{-9} - Cz^{-3}. \tag{4}$$

This form (used in much previous work on wetting[13]) captures the key aspects of the potential and includes parameters that are relatively well known in many cases: D is the well depth and C is the strength of the van der Waals asymptotic interaction.[14,15] For this potential the equilibrium distance is

$$z_m = [2C/(3D)]^{1/3}. \tag{5}$$

The net potential in the slab geometry is taken to be the sum of the respective contributions of the two surfaces

$$V_{\text{slab}}(z) = V(z) + V(L-z). \tag{6}$$

This assumption of additivity of the two contributions omits many-body effects that would reduce the overall attraction.[16]

As with the functional form assumed for $V(z)$, we oversimplify the description in order to derive qualitative predictions.

The adsorption behavior is to be predicted by evaluating the equilibrium number of atoms adsorbed per unit area N as a function of the chemical potential μ, the value of N and other thermodynamic properties may be determined by minimizing (as a function of the variable N) the grand potential energy per unit area

$$\Omega(N)=F(N)-\mu N, \tag{7}$$

where F is the Helmholtz free energy per unit area. The value of the temperature is implicitly present in both Ω and F.

In this paper we explore density-functional (DF) models of quantum fluids at temperature $T=0$.[17–22] The DF method allows a detailed and reliable study of the film structure and energetic. Typically, the uncertainty in the predicted energies arising from inadequate knowledge of the adsorption potential. In fact, this model has been used successfully to predict wetting behavior of quantum fluids on various surfaces.[18–20]

II. ^{3}He CALCULATIONS

The DF method employed here is that used by Calbi and Hernández to treat ^{3}He adsorption on graphite.[18] The total energy of the system is expressed in terms of the density $\rho(\vec{r})$ as follows,

$$E[\rho]=E_0[\rho]+\int d^3r V_{\text{slab}}(z)\rho(\vec{r}). \tag{8}$$

The functional $E_0[\rho]$ is the putative energy of a hypothetical nonuniform fluid in the absence of an external potential field. This functional is constructed phenomenologically so as to be both plausible and consistent with known properties of the bulk system (i.e., equilibrium density, energy, and compressibility). Its properties and justification are discussed by Calbi and Hernández.[18] The density function $\rho(\vec{r})$ is

$$\rho(\vec{r})=2\sum_i |\phi_i(\vec{r})|^2, \tag{9}$$

where ϕ_i are the single particle (sp) states that comprise the ground state, taken as a Slater determinant. We consider that these sp states have the form

$$\phi_{k_\parallel \nu}(r_\parallel,z)=\frac{1}{\sqrt{A}}e^{ik_\parallel\cdot r_\parallel}f_{k_\parallel\nu}(z), \tag{10}$$

where $k_\parallel$ and $r_\parallel$ are the projections of the wave vector $\vec{k}$ and the position $\vec{r}$ in the plane parallel to the substrate. The functions $f_{k_\parallel\nu}(z)$ are the self-consistent solutions of a mean-field equation derived from the minimization of the energy $E[\rho]$.

In our calculations we have exposed the He fluid to various adsorbing surfaces separated by variable distance L. It is important to realize how large is the difference in $V(z)$ provided by different adsorption surfaces. Here we restrict our attention to three surfaces that vary between weakly attractive to moderately attractive. Figure 1 displays the three distinct potentials we consider, in the case $L=12$ Å. The parameters used in these calculations are reported in GCC and are based on the most recent *ab initio* potential calculations.[14,15] They vary between the weakly attractive case of Cs (the most inert adsorption surface known for He), the somewhat more attractive Li case, and the more typical case of a Au surface. Note also that the hard-core region of exchange repulsion is much more extended in the alkali-metal cases than for Au. Specifically, z_m is 4.55 Å for ^{3}He on Cs, but only 2.66 Å on Au.[3] Hence the available adsorption volume (for given value of L) is smaller in the former than in the latter cases. This can yield dramatic consequences when L is small.

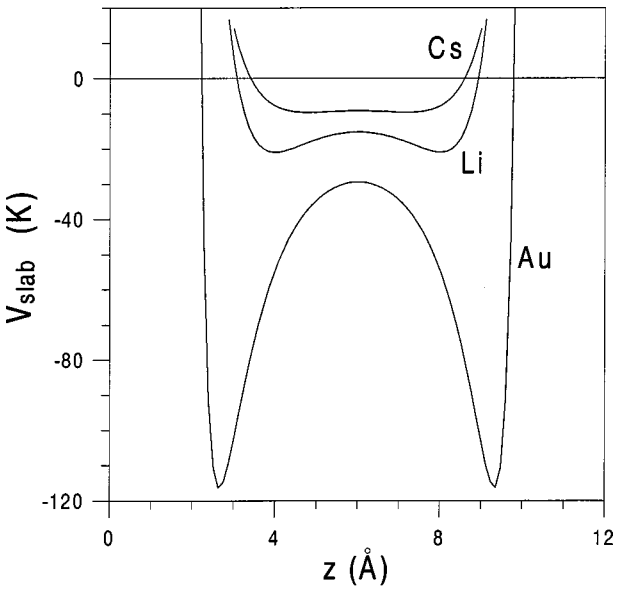

FIG. 1. Adsorption potentials of ^{3}He on various surfaces for the case of separation $L=12$ Å. The potentials parameters and sources are discussed in the text.

The first system to be discussed is ^{3}He confinement between Cs surfaces. These results are of particular interest because ^{3}He exhibits a prewetting transition at low T on Cs.[23] The present functional succeeds well in describing that transition on a single surface,[24] so we are optimistic about its accuracy here. Figure 2 exhibits the dependence of μ on total density N (number per unit area) for various separations L. The case $L=10$ Å reveals a monotonic very rapid variation. The reason is that the He is narrowly confined by the nearly hard walls of Cs, forming a compressed quasimonolayer; Fig. 3 compares this layer's density with that obtained for a monolayer of a single surface of graphite. The latter is somewhat more localized due to the very deep adsorption potential on that surface. Indeed, the graphite case yields the most localized ^{3}He of any single surface because it provides the deepest potential.[15]

As L increases, the calculated behavior changes qualitatively. For $L=15$ Å, the dependence of μ on N is seen in Fig. 2 to be nonmonotonic. This indicates the presence of a transition, requiring a Maxwell construction to find the equilibrium behavior. The results are shown in Fig. 4. For the cases 20 Å $\geqslant L>10$ Å the coverage jumps from zero to a multilayer capillary condensed fluid, which fills the available space. Figure 5 shows the evolution of the density profile, including the metastable (or unstable) solutions for which the

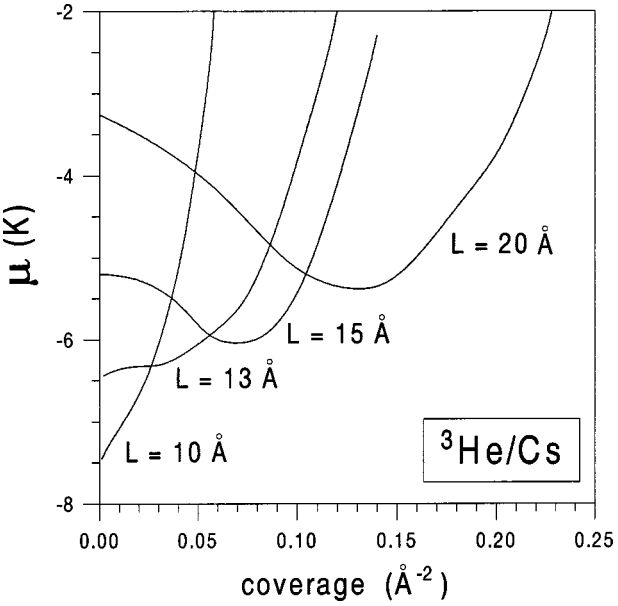

FIG. 2. Chemical potential of ^{3}He as a function of coverage, for various separations L between Cs surfaces.

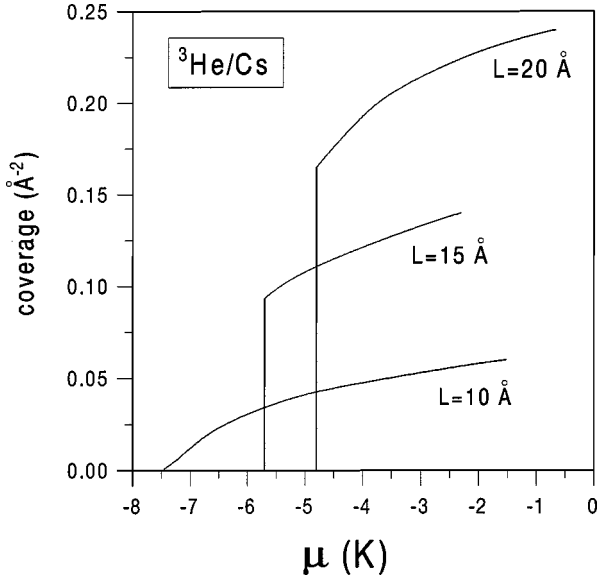

FIG. 4. Coverage as a function of μ for various L values; as discussed in the text these are derived from data in Fig. 2 by Maxwell constructions.

density grows continuously and relatively smoothly throughout the available space. The layering structure manifested at the highest density seen in Fig. 5 is very sensitive to the value of L. This dependence, which we have not explored in detail, implies that there exists an oscillatory force between the Cs surfaces, as would be manifested in an atomic force microscopy (AFM) experiment. We have not computed this behavior because the use of such low T AFM's is unlikely in the near future. We hope that this pessimism is not justified.

For very large L ($L>40$ Å), although there is a transition to a CC phase, the adsorption at low coverages resembles the single-surface prewetting, as is seen in Figs. 6 and 7 for $L=45$ Å: the fluid behaves as a film at low coverages and eventually ''sees'' the other surface as the chemical potential approaches its value at saturation.

Figures 8–10 present analogous results for adsorption isotherms on Li, beginning with $L=15$ Å. At 15 Å, the coverage jumps from zero to about one layer of ^{3}He. At $L=20$ and 24 Å, instead, a film forms prior to this transition. The key difference relative to Cs is thus the presence of the thin-film regime. The density profiles of the film and CC phases for $L=20$ Å are shown in Fig. 10, where the dotted lines are metastable solutions.

Finally, we turn to the much more attractive case of Au, that we illustrate in Figs. 11 and 12. A low-density phase is found for $L\leqslant 8$ Å, while for $L=9$ Å there is a transition to a bilayer phase, the density evolution of which is shown in Fig. 12. This regime disappears as soon as L is sufficiently large, $L\geqslant 10$ Å, where we find a continuously growing film. It is important to mention that due to the strong attraction of

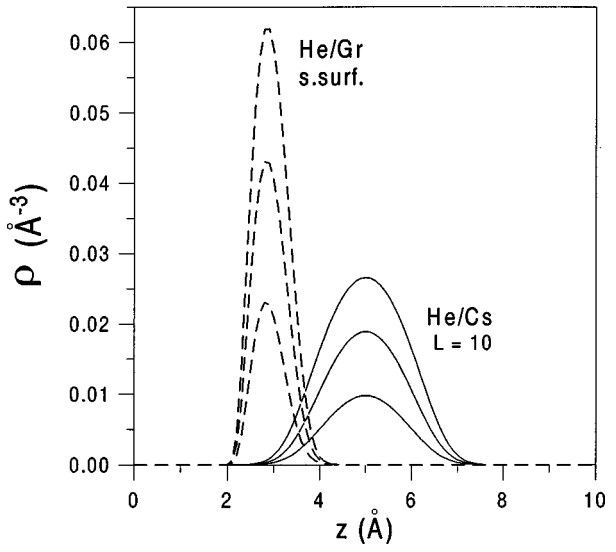

FIG. 3. Comparison between density profiles of ^{3}He between Cs surfaces ($L=10$ Å, full curves at densities 0.02, 0.04, and 0.06 Å^{-2}) and of a monolayer on a single surface of graphite (dashed curve, from Ref. 18).

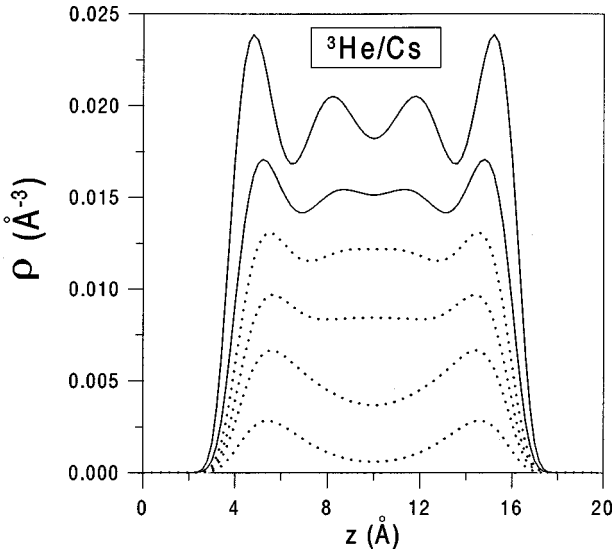

FIG. 5. ^{3}He densities for Cs, $L=20$ Å and coverages 0.02, 0.06, 0.1, 0.14, 0.18, and 0.24 Å^{-2}. Dotted curves are metastable solutions.

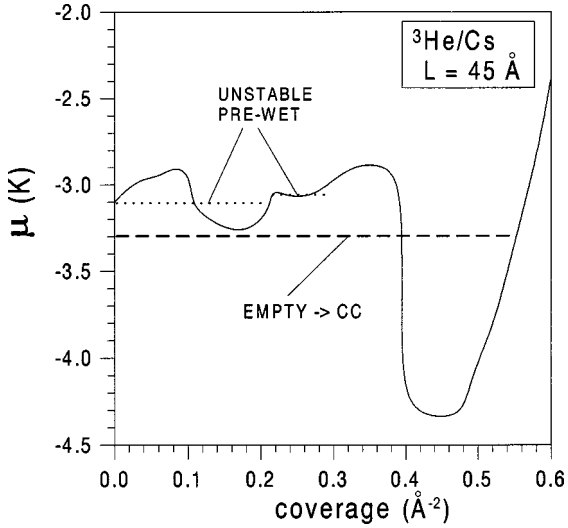

FIG. 6. Chemical potential of ^{3}He between Cs surfaces separated $L=45$ Å as a function of coverage. Dotted and dashed lines are derived by Maxwell constructions for the unstable prewetting and empty-to-CC transitions, respectively.

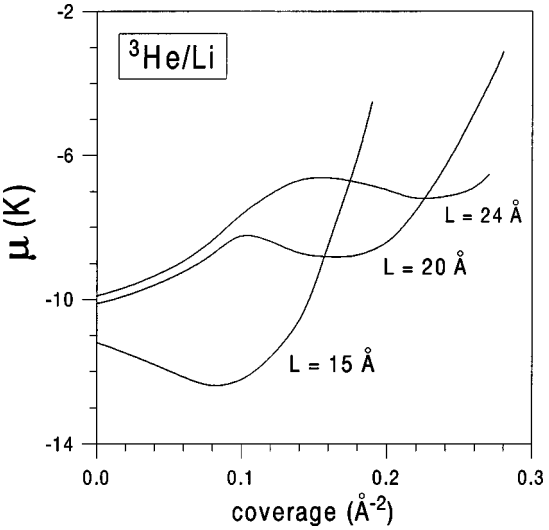

FIG. 8. Chemical potential as a function of coverage between Li surfaces at various separations.

the substrate, when the coverage is high enough the formed layers become very dense. In this situation the density reaches values that are beyond the range of validity of the DF. We think that it is very likely that the first layer solidifies below saturation (like the case of ^{3}He on a single surface of graphite) and that the film-to-CC transition involves the atoms situated in a second layer. This behavior cannot be described with this DF.

The transitions predicted by the DF theory are in good agreement with the GCC model. For the case of Cs, the DF results are summarized in Table I, where we show the values of the chemical potential μ at which the transitions occur for the different separations L. To facilitate the comparison with the predictions of the GCC model, we have also shown the reduced quantities Δ and L^*. Comparing the values of Δ and L^* in this table and Fig. 3 from Ref. 3 we can see that the CC prediction of the simple model is consistent with the present calculations in several respects. For small L^* the transition occurs at values of μ that agree well with the predictions of the model. This is remarkable and perhaps fortuitous in view of the fact that the available volume is essentially that of a bilayer film, for which the macroscopic description should be ill suited.

For ^{3}He in Li, again the comparison with the simple model is rather favorable (see Fig. 4, Ref. 3). Note that the range of L^* values that exhibit no film is much narrower than the preceding case of Cs. Remarkably, the transition behavior corresponds to the prediction insofar as the $L=15$ Å jump occurs close to the predicted value of μ. Further, the points corresponding to film and/or CC transitions agree with the μ values predicted by the simple model.

Finally, for the case of ^{3}He on Au the results are displayed in Table II. The simple model's prediction of the empty-to-film transition is consistent with DF results (see the Table and Fig. 5, Ref. 3). The CC phase is replaced in the DF

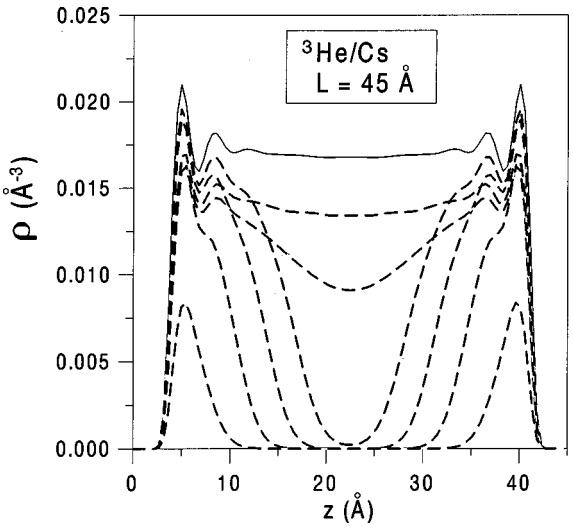

FIG. 7. Density profiles of ^{3}He between Cs surfaces ($L=45$ Å) at densities 0.06, 0.18, 0.28, 0.37, 0.42, 0.49, and 0.6 Å^{-2}. Dashed curves are metastable solutions.

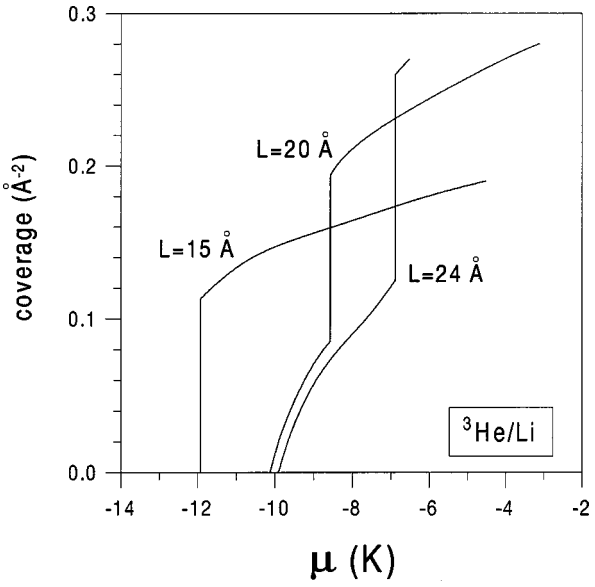

FIG. 9. Adsorption isotherms on Li, derived from Fig. 8.

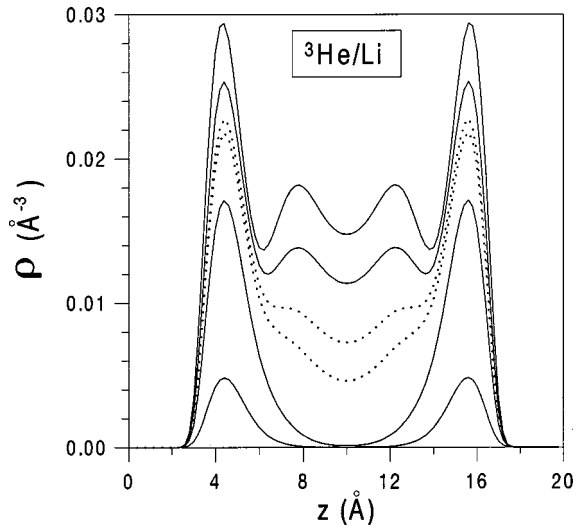

FIG. 10. Density as a function of distance for $L=20$ Å on Li. Dotted curves are not stable.

calculations by a very inhomogeneous configuration with an empty space in the middle of the slab (see Fig. 12), that we call the ''bilayer phase.'' This takes place in a narrow domain of L (8 Å $<L<$10 Å), as expected for the CC phase in the simple-model description. The low-density phase found for $L=7$ Å ($L^*=2.6$), corresponds to the transition to the empty phase predicted at $L^*=2$ by the simple model. The same can be stated in the case of the Cs surfaces separated by $L=10$ Å, ($L^*=2.2$). The film-to-CC transition is not described by this method because that appears very close to saturation, at coverage values beyond the domain of the DF.

III. ^{4}He CALCULATIONS

To treat ^{4}He, again in the DF scheme of Eq. (8), we choose for the phenomenological energy functional $E_0(\rho)$ the form originally proposed by Dupont-Roc *et al.*,[17] which

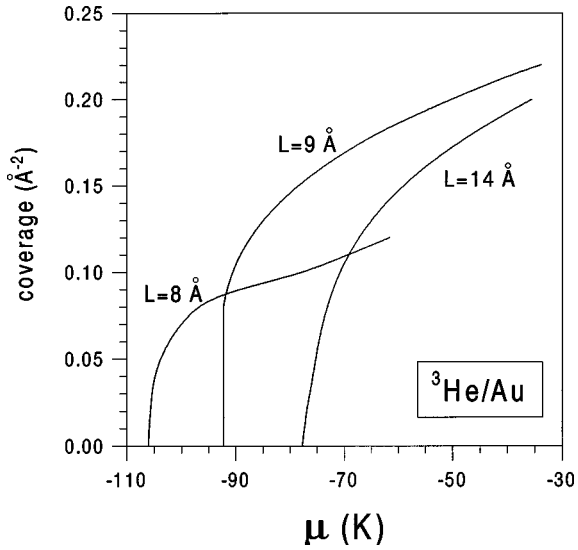

FIG. 11. Adsorption isotherms for ^{3}He between Au surfaces separated by various distances. Only for $L=9$ Å is discontinuous behavior found.

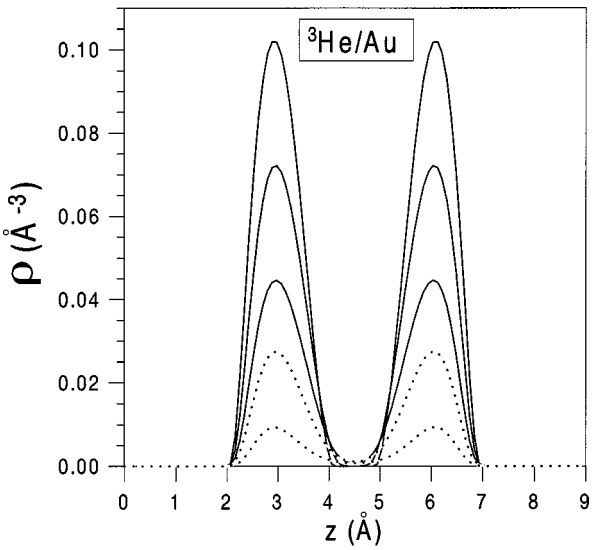

FIG. 12. Density profiles for ^{3}He within Au at $L=9$ Å. The curves shown correspond to coverages 0.02, 0.06, 0.1, 0.16, and 0.22 Å^{-2}.

has been extensively used to study static and dynamical properties of inhomogeneous phases of liquid ^{4}He (surfaces, droplets, films, etc.).

The functional of Ref. 17 is known to give a good description of the $T=0$ equation of state, of the static density-density response function of the bulk liquid, and of the properties of the free surface of liquid ^{4}He. It has been used in a variety of calculations, ranging from the study of impurities[25] and electrons[26] in bulk ^{4}He, to alkali atom adsorption on the surface of liquid ^{4}He (Ref. 27) and wetting phenomena on alkali-covered substrates.[20] For a detailed description of this functional we refer the reader to Ref. 17.

This functional has been slightly revised[19] and supplemented by an extra term depending on the gradient of the liquid density so to correctly reproduce also the static structure factor and the bulk dispersion relations of sound excitations in liquid ^{4}He. This extended functional has been applied to the study of density oscillations in ^{4}He clusters,[29] of surface excitations in ^{4}He films [19,30] and of other related dynamical phenomena.[28] The phase diagram of ^{4}He between two Li surfaces has been calculated using both functionals, to check the differences. Since for a given L^* the values of Δ at the phase boundaries in the diagram reported in Fig. 15 do not differ by more than 5% but the computer time required to minimize the new functional increases by almost an order of magnitude when using the new functional, we have

TABLE I. Values of the chemical potential μ at which the transitions occur for each separation L, for ^{3}He in a slab of Cs. Also shown are the reduced quantities Δ and L^*, defined in the text.

μ (K)	L (Å)	Δ	L^*
−7.5	10	3.2	2.2
−6.4	13	2.5	1.9
−5.7	15	2.1	3.3
−4.8	20	1.5	4.4
−3.3	45	0.5	9.9

TABLE II. Same as Table I, for ^{3}He in a slab of Au.

μ (K)	L (Å)	Δ	L^*
−134	7	50.2	2.6
−106	8	39.6	3.0
−92.3	9	34.3	3.3
−85.1	10	31.6	3.7
−80.0	12	29.6	4.4
−77.5	14	28.7	5.2
−76.6	17	28.3	6.3
−76.0	20	28.1	7.4

decided to perform extensive calculations on several substrates with the old functional.

To evaluate $V_{\rm slab}(z)$ we have used the most recent ^{4}He/alkali potentials given in Ref. 14

In the case of interest here, of a slab geometry with planar surfaces, the minimization of Eq. (8) leads to the equation

$$\left(-\frac{\hbar^2}{2M}\nabla^2+U[\rho(z)]\right)\sqrt{\rho(z)}=\mu\sqrt{\rho(z)}, \qquad (11)$$

where the effective potential U is defined as $U[\rho(z)] \equiv \delta E_0[\rho(z)]/\delta\rho(z)+V_{\rm slab}(z)$, and μ is a Lagrange multiplier, which may be identified with the chemical potential, and whose value is fixed by the normalization condition

$$\int_0^L \rho(z)dz=N/A. \qquad (12)$$

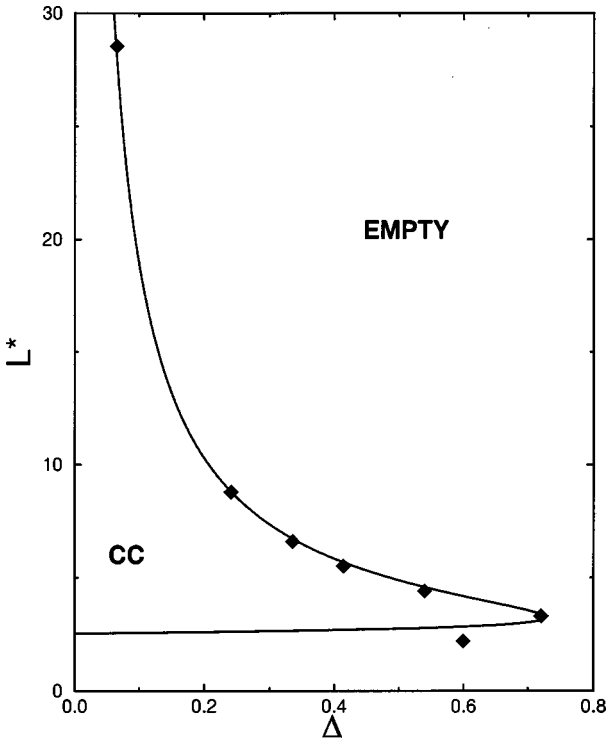

FIG. 13. Predictions for ^{4}He in Cs ($D^*=5.4$, $z_m=4.55$ Å) obtained with the simple GCC model of transitions empty-to-film or filled pore (CC) (full curves) compared with transition results found from DF theory, present work (full diamonds).

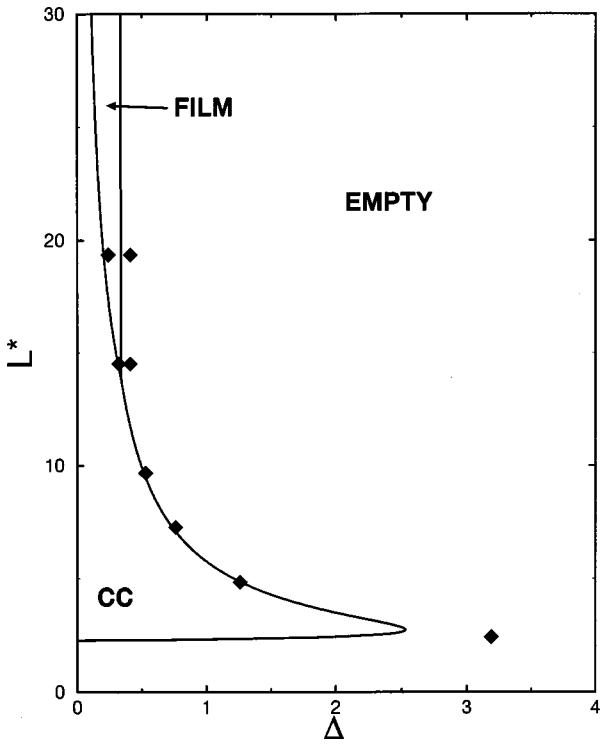

FIG. 14. Same as Fig. 13 for ^{4}He in Na ($D^*=8.9$, $z_m=4.13$ Å).

Imposing the boundary conditions: $\rho(0)=\rho(L)=0$, this equation may easily be solved numerically thus providing the ground-state eigenvalue μ corresponding to a given N/A.

Figures 13 to 16 show the comparison of the DF calculation and the GCC model's results. In Fig. 13 we show the situation of ^{4}He on Cs. As predicted there is no film phase in

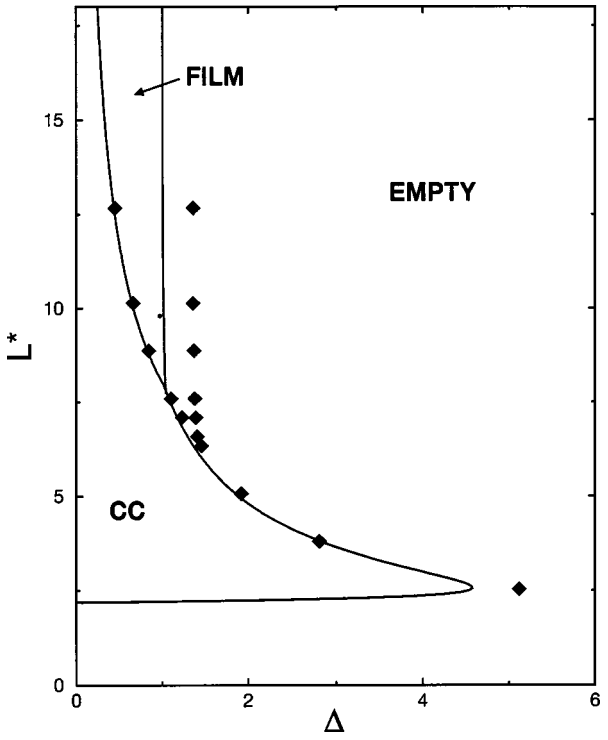

FIG. 15. Same as Fig. 13 for ^{4}He in Li ($D^*=12$, $z_m=3.95$ Å).

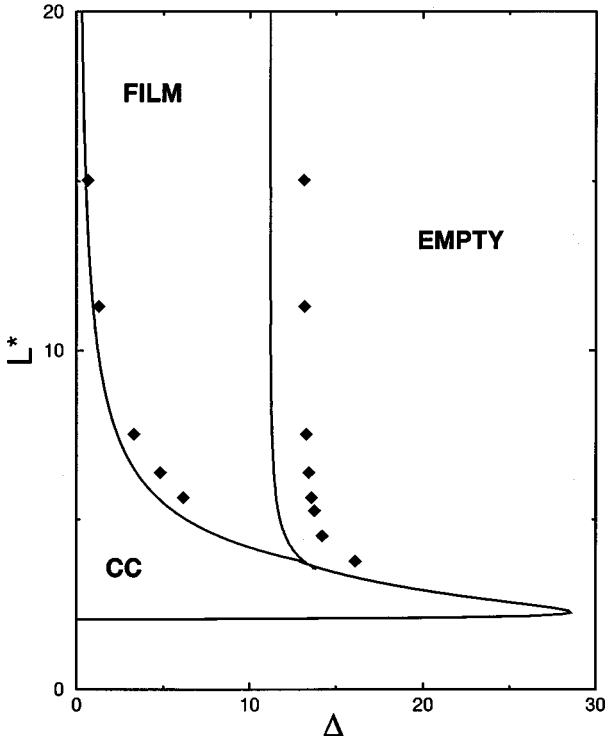

FIG. 16. Same as Fig. 13 for ^{4}He in Au ($D^*=42$, $z_m=2.7$ Å).

this case, and as we can see the empty-to-CC phase transition obtained with the DF agree well with the phase diagram obtained with the simple model.

Figure 14 displays the phase diagram for ^{4}He on Na, notice that it is very similar to ^{3}He on Cs since the values of D^* are 8.79 and 9.42, respectively. The DF method yields the empty-to-film, film-to-CC, and empty-to-CC transitions that are in good agreement with the predictions as indicated in the figure.

The case of ^{4}He on Li is shown in Fig. 15, where we can see that the comparison is satisfactory, even though according to the DF the empty-to-film transition occurs at a higher Δ. The same situation is found for ^{4}He on Au, which is shown in Fig. 16.

IV. SUMMARY

The present calculations indicate that the simple model presented by GCC is generally in good agreement with detailed microscopic calculations for the He isotopes. The agreement, although not universal, occurs even in some instances where it might not be expected to succeed, such as the case of small separations L. What remains to be seen is whether experimental data for these cases and calculations and measurements for more classical systems also correspond to the model's predictions. Of course, the calculations are more readily achieved than experiments insofar as the greatest interest arises in those instances of small L where the parallel surface assumption is hard to realize experimentally.

Laboratory experiments with porous media are typically done with heterogeneous surfaces. A future direction for our research is an attempt to generalize the GCC model to such very important cases. Another direction is the study of carbon nanotubes, for which heterogeneity seems not to be a critical problem; instead one needs to explore the validity of the model for a nearly cylindrical environment having a nanometer scale diameter.

We are grateful to Mary J. Bojan and Moses Chan for helpful discussions. This research was supported by the Army Research Office, the National Science Foundation, and the Petroleum Research Fund of the American Chemical Society.

*Electronic address: mwc@psu.edu

[1] B. V. Derjaguin, Acta Physicochim. URSS **12**, 181 (1940).
[2] S. J. Gregg and K. S. W. Sing, *Adsorption, Surface Area and Porosity*, 2nd. ed. (Academic, London, 1982).
[3] S. M. Gatica, M. Calbi, and M. W. Cole, Phys. Rev. E **59**, 4484 (1999).
[4] M. J. Bojan, E. Cheng, M. W. Cole, and W. A. Steele, Adsorption **2**, 51 (1996); M. J. Bojan and W. A. Steel, Carbon (to be published).
[5] R. Evans, in *Liquids at Interfaces*, edited by J. Charvolin, J. F. Joanny, and J. Zinn-Justin (Elsevier, Amsterdam, 1990).
[6] R. F. Cracknell, D. Nicholson, and N. Quirke, J. Chem. Soc., Faraday Trans. **90**, 1487 (1994); K. E. Gubbins, M. Sliwinska-Bartokwiak, and S. H. Suh, Mol. Simul. **17**, 333 (1996).
[7] B. K. Peterson, K. E. Gubbins, G. S. Helfinger, U. M. B. Marconi, and F. Van Swol, J. Chem. Phys. **88**, 6487 (1988).
[8] K. M. Godshalk and R. B. Hallok, Phys. Rev. B **36**, 8294 (1987).
[9] E. Cheng, M. R. Swift, and M. W. Cole, J. Chem. Phys. **99**, 4064 (1993).
[10] M. J. Bojan, R. V. Slooten, and W. A. Steele, Sep. Sci. Technol. **27**, 1837 (1992).
[11] Q. Wang and J. K. Johnson, Int. J. Thermophys. **19**, 835 (1998); Mol. Phys. **95**, 299 (1998).
[12] E. Cheng, M. W. Cole, W. F. Saam, and J. Treiner, Phys. Rev. B **48**, 18 214 (1993).
[13] J. S. Rowlinson and B. Widom, *Molecular Theory of Capillarity* (Clarendon Press, Oxford, 1989).
[14] A. Chizmeshya, M. W. Cole, and E. Zaremba, J. Low Temp. Phys. **110**, 677 (1998).
[15] G. Vidali, G. Ihm, H. Y. Kim, and M. W. Cole, Surf. Sci. Rep. **12**, 133 (1991).
[16] Nonadditive corrections should be small, as discussed in M. Schmeits and A. A. Lucas, Prog. Surf. Sci. **14**, 1 (1983); and L. W. Bruch, M. W. Cole, and E. Zaremba, *Physical Adsorption: Forces and Phenomena* (Oxford Univ. Press, Oxford, 1997).
[17] J. Dupont-Roc, M. Himbert, N. Pavloff, and J. Treiner, J. Low Temp. Phys. **81**, 31 (1990).
[18] M. M. Calbi and E. S. Hernández, Phys. Rev. B **57**, 13 258 (1998).
[19] L. Pricaupenko and J. Treiner, J. Low Temp. Phys. **96**, 19 (1994).
[20] E. Cheng, M. W. Cole, J. Dupont-Roc, W. F. Saam, and J. Treiner, Rev. Mod. Phys. **65**, 557 (1993).
[21] S. Stringari and J. Treiner, Phys. Rev. B **36**, 8369 (1987).
[22] M. Barranco, M. Pi, S. M. Gatica, E. S. Hernández, and J. Navarro, Phys. Rev. B **56**, 8997 (1997).

[23] D. Ross, J. A. Phillips, and P. Taborek, J. Low Temp. Phys. **95**, 405 (1994).
[24] M. M. Calbi (unpublished).
[25] F. Dalfovo, Z. Phys. D **29**, 61 (1994).
[26] F. Ancilotto and F. Toigo, Phys. Rev. B **50**, 12 820 (1994).
[27] F. Ancilotto, E. Cheng, M. W. Cole, and F. Toigo, Phys. Rev. B **98**, 323 (1995).
[28] F. Dalfovo, A. Franchetti, A. Lastri, L. Pitaevskii, and S. Stringari, Phys. Rev. Lett. **75**, 2510 (1995); J. Low Temp. Phys. **104**, 367 (1996).
[29] M. Casas, F. Dalfovo, A. Lastri, Ll. Serra, and S. Stringari, Z. Phys. D **35**, 67 (1995).
[30] A. Lastri, F. Dalfovo, L. Pitaevskii, and S. Stringari, J. Low Temp. Phys. **98**, 227 (1995).